# Features of Electro-magnetic Methods for Evaluating Sizes of Surface Cracks in Metals

Dorian Asenov Minkov

*Abstract* – **Two methods are described for evaluating sizes of surface cracks in metals. In the first method, induced leakage magnetic field around a surface crack, measurement and calculation of Hall voltage from Hall element, and minimization of the deviation between such voltages for several locations of the Hall element are used. In the second method, induced AC current on the metal surface, and loop antenna with output voltage, depending on the amplitude of the magnetic field within the crack are used.**

*Keywords* – **Electro-magnetic methods, evaluating depths of surface cracks in metals, Hall element, loop antenna**

## I. INTRODUCTION

Presence of surface cracks in materials can lead to their mechanical breakdown, especially under heavy load or in hostile environment. Evaluating the depths of surface cracks is difficult, because the small crack width often hinders the applicability of direct visualization techniques. Development of methods for evaluating sizes (also called 'sizing') of cracks on metal surfaces is important, because they are needed for prediction and prevention of failure of equipment for the pipeline, railway and aircraft industries.

In this paper, two electro-magnetic methods for non-destructive sizing of surface cracks in metals are outlined. These methods were developed, with my active participation, during my five years work at the Fracture Research Institute in Sendai, Japan.

## II. METHOD USING MEASUREMENTS BY A HALL ELEMENT

### A. Description of the method

In this method, a magnetic metal is magnetized, by a static magnetic field, parallel to its flat surface. The magnetic field redistributes around a surface crack, and its part called 'leakage magnetic field' (LMF) spreads out of the specimen, in the vicinity of the crack. Hall voltage is measured by a Hall element, and is proportional to LMF.

LMF is also estimated using the 'dipole model of a crack' (DMC). In DMC, the crack is considered to be filled with magnetic dipoles oriented parallel to the magnetizing field, the opposite poles being located on the two opposite walls of the crack. Integrating the contributions of all of these magnetic dipoles, gives LMF in a given point outside the specimen. Hall voltage is calculated by summing its constituents over the active region of the Hall element.

Sizes of the crack are evaluated by minimizing the RMS deviation between the set of measured Hall voltages and a set of calculated Hall voltages, in the vicinity of the crack.

D. Minkov is with the College of Energy and Electronics, Technical University - Sofia, bul. Bulgaria 31, 2140 Botevgrad, Bulgaria, e-mail: d.minkov@tu-sofia.bg

We investigated only cracks with constant widths. The magnetizing field was always directed perpendicular to the long axis $y$ of the crack, at the metal surface. The density of the magnetic dipoles was assumed to increase linearly with the depth of the crack. The Hall voltages were measured along scanning lines parallel to the magnetizing field.

### B. Formulation of the method

Let us consider the simplest possible surface crack representing a right angle parallelepiped, with length $2l$ along the $y$-axis, width $2a$ and depth $d$. The $(x0y)$ plane of the coordinate system is at the flat metal surface, the point 0 is at the geometrical center of the crack in this plane, and the z-axis is directed away from the metal. In case of magnetizing the metal parallel to its crack containing surface, magnetic field lines in the vicinity of such a crack, and a representation of LMF by only one magnetic dipole in the DMC framework are illustrated in Fig. 1.

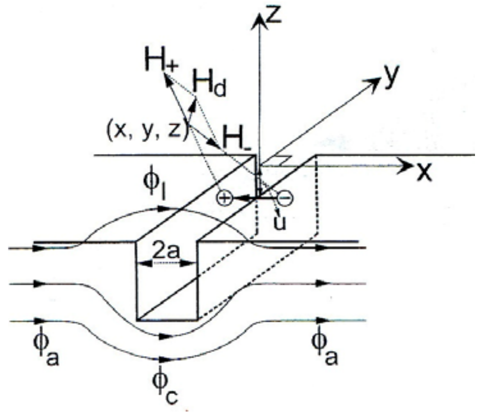


Fig. 1. LMF $H_d$ for only one magnetic dipole has two components $H_+$ and $H_-$ . $u$ is distance between this dipole and the metal surface

The z-component of the intensity of the leakage magnetic field (ZILMF) of this crack is represented by integrating the ZILMF of all of the dipoles filling the crack:

$$H_{rz}(x,y,z)=\int_{-l-y}^{l-y}\int_{0}^{d}\frac{m(u)}{4\pi\mu_0}\left\{\frac{(z+u)(\mathrm{d}u)(\mathrm{d}y)}{\left[(x+a)^2+y^2+(z+u)^2\right]^{\frac{3}{2}}}-\frac{(z+u)(\mathrm{d}u)(\mathrm{d}y)}{\left[(x-a)^2+y^2+(z+u)^2\right]^{\frac{3}{2}}}\right\} \quad (1)$$

where $m(u)$ is the surface density of magnetic dipoles at the crack walls. It is assumed that:

$$m(u)|_{u\subset[0,d]}=m(\nu)|_{\nu=u/d\subset[0,1]}=m_1+m_2\nu \quad (2)$$

where $m_1$ and $m_2$ are constants. At the crack mouth $m(0)=m_1$ , and the crack bottom $m(d)= m_2$ [1].

Performing the integration in (1) gives:

$$H_{rz}(x,y,z)=\frac{m_2}{4\pi\mu_0 d}$$
$$\times\left\{\begin{array}{l}\left(\frac{m_1 d}{m_2}-z\right)\left[\begin{array}{l}A_1(l-y,x+a)+A_1(l+y,x+a)\\-A_1(l-y,x-a)-A_1(l+y,x-a)\end{array}\right]\\+\left[\begin{array}{l}-(x+a)A_2(l-y,x+a)-(x+a)A_2(l+y,x+a)\\+(x-a)A_2(l-y,x-a)+(x-a)A_2(l+y,x-a)\end{array}\right]\\+\left[\begin{array}{l}(l-y)A_3(l-y,x+a)+(l+y)A_3(l+y,x+a)\\-(l-y)A_3(l-y,x-a)-(l+y)A_3(l+y,x-a)\end{array}\right]\end{array}\right\}$$
$$A_1(l-y,x-a)=\ln\left[\sqrt{\frac{(x-a)^2+(z+d)^2}{(x-a)^2+z^2}}\times\frac{(l-y)+\sqrt{(x-a)^2+(l-y)^2+z^2}}{(l-y)+\sqrt{(x-a)^2+(l-y)^2+(z+d)^2}}\right],$$
$$A_2(l-y,x-a)=\tan^{-1}[A_{21}(l-y,x-a)],$$
$$A_{21}(l-y,x-a)=\frac{(l-y)(x-a)\left[(z+d)\sqrt{(x-a)^2+(l-y)^2+z^2}-z\sqrt{(x-a)^2+(l-y)^2+(z+d)^2}\right]}{(x-a)^2\sqrt{(x-a)^2+(l-y)^2+z^2}\times\sqrt{(x-a)^2+(l-y)^2+(z+d)^2}+(l-y)^2 z(z+d)},$$
$$A_3(l-y,x-a)=\ln\left[\frac{\sqrt{(x-a)^2+(l-y)^2+(z+d)^2}+z+d}{\sqrt{(x-a)^2+(l-y)^2+z^2}+z}\right]. \qquad (3)$$

where $\mu_0$ is vacuum permeability, $A_j(l-y,x+a)$, $A_j(l+y,x-a)$ and $A_j(l+y,x+a)$ for $j=1,2,3$ are obtained by replacing respectively $x-a$ by $x+a$, $l-y$ by $l+y$ and both $l-y$ by $l+y$ and $x-a$ by $x+a$ in the above expressions for $A_j(l-y,x-a)$.

For a crack with a length $2l_0$ and an arbitrary depth profile, along the long axis of the crack, according to DMC, ZILMF for such a crack is:

$$H_z(x,y,z)=\sum_{i=l}^{N_1N_2}H_{rz}(x,y_i,z)=\sum_{i=l}^{N_1N_2}H_{rz}(x,y-l_i,z) \qquad (4)$$

where $i$ is the number of a constituent sub-crack, and $l_i=-l_0[1-(2i-1)/(N_1N_2)]$ .

A Hall element is positioned on the flat metal surface. Its Hall voltage is formulated, by integrating ZILMF over the active region of the element, as follows:

$$V_H(x,y,z)=\frac{\mu_0 I}{qnd_a}\frac{\sum_{i_1=1}^{n_1}\sum_{i_2=1}^{n_1}\sum_{i_3=1}^{n_2}H_z(x_{i_1},y_{i_2},z_{i_3})}{n_1^2n_2}=\left(\frac{\mu_0 I}{qnd_a}H_a\right)=cH_a \qquad (5)$$

where $I$ is the electric current supplied between two opposite contacts of the Hall element, $V_H(x,y,z)$ is the Hall voltage induced between the other two opposite contacts, $d_a$ is the thickness of the active layer of the chip of the Hall element, $q$ is the absolute value of the electron charge, $n$ is the electron concentration in the active layer which is assumed to be n-type and to have square-shaped top surface of its active region, the volume of the active region is represented as a sum of $n_1^2n_2$ parallelepipeds, $n_1$ and $n_2$ are the numbers of these parallelepipeds along the length and the thickness of the active region, $H_z(x_{i1},y_{i2},z_{i3})$ is the z-component of the intensity of the leakage magnetic field of the investigated crack with an arbitrary depth profile in the center of the parallelepiped with number $(i_1,i_2,i_3)$, $H_a$ is the average value of ZILMF over the volume of the active region of the Hall element, and $c=\mu_0 I/(qnd_a)$ is constant.

During measurement, the top planar surface of the Hall element is positioned onto the metal surface. The Hall voltage is measured at several locations, close to the crack, which are usually aligned along a scanning line parallel to the magnetizing field [2].

The Hall voltage is also calculated for each of the measurement locations by using Eqns. 1 to 5. The unknown depth profile of the crack, the width of the crack and the depth distribution of $m$ can be computed by minimizing the RMS deviation $\sqrt{\left\{\sum_{i=1}^{N}\left[V_H^m(i)-V_H^c(i)\right]^2\right\}/N}$ between the set $V_H^m(i)$ of measured Hall voltages, and its respective set $V_H^c(i)$ of calculated Hall voltages, where $N$ is the number of measurement points. This technique is a 'crack inversion'.

*C. Results*

In the discussed experiments were used right angle parallelepiped specimens of ferromagnetic steel SS400 with dimensions 200x100x5 mm. One surface crack with a constant width of $2a$ = 0.9 mm is cut mechanically at the surface of each specimen, and the crack length is $2l_0$ = 10 mm. One crack has a right angle parallelepiped shape, and is designated by a first symbol "r" in the case symbol, which describes the measurement conditions. The other crack has an isosceles triangular depth profile, and is designated by a first symbol "t" in the case symbol.

The Hall voltage is measured by a Toshiba THS124 GaAs Hall element, supplied with DC current $I$ = 5 mA, which leads to $c = 2.096\times10^{-6}$ Ω.m in Eq. 5. The size of the active region of the chip is 125x125x6 µm, and the distance between the center of this active region and the metal surface is $z_m$ = 0.54 mm.

One set of measured Hall voltages is obtained along a scanning line passing through 0, and is designated by a second symbol "c" in the case symbol. Other set of measured Hall voltages is obtained along a scanning line at a distance of $2l_0/3$ = 3.33 mm from the first scanning line, and is designated by a second symbol "s" in the case symbol. A second symbol "b" means that both "c" and "s" sets of measurements are used. All of the Hall voltage measurements are taken on the same side with respect to the long axis of the crack, and the number of measurement points along each of the scanning lines is $N$ = 10.

Two types of crack inversions are performed. In the first type, the crack is assumed to have a right angle parallelepiped shape, and $N_1N_2$ = 1. The inversions give the parameters $d$, $a$, $m_1$, $m_2$. The depth $d$ for the triangular depth profile crack is expressed by the depth $d_e$ of a crack with a semi-ellipsoidal depth profile and the same area below its long axis whereat $d_e = 4d/\pi$, which represents similarly the maximum depth $d_m = d_{tr}$ (true depth) of the investigated crack. The inversion results are shown in Table 1.

The second type of crack inversions is performed for the triangular depth profile crack only. It is assumed that the depth profile of the crack is unknown but symmetrical with respect to the central axis, as well as that the crack width is measured independently. Both the true and the computed depth profiles for $N_1$ = 4 and $N_2$ = 7 are illustrated in Fig. 2.

TABLE 1. RESULTS FROM FIRST TYPE CRACK INVERSIONS

| Case Sym-bol | $m_1$ $\left[\frac{H.A}{m^2}\right]$ | $m_2$ $\left[\frac{H.A}{m^2}\right]$ | $d$ [mm] | a [mm] | $\frac{\lvert d-d_{tr}\rvert}{d_{tr}}$ [%] | $\frac{\lvert a-a_{tr}\rvert}{a_{tr}}$ [%] |
|---|---|---|---|---|---|---|
| rc2 | 0.45 | 0.99 | 2.690 | 0.480 | 10.33 | 6.67 |
| rs2 | 0.61 | 0.99 | 3.184 | 0.395 | 9.20 | 12.22 |
| rb2 | 0.42 | 0.83 | 2.810 | 0.477 | 10.73 | 11.00 |
| tc2 | 0.42 | 0.26 | 2.802 | 0.405 | 6.60 | 10.00 |
| ts2 | 0.42 | 0.26 | 2.889 | 0.407 | 3.70 | 9.56 |
| tb2 | 0.42 | 0.26 | 2.799 | 0.407 | 6.70 | 10.56 |

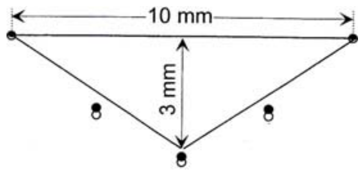


Fig. 2. True and computed depth profiles for the crack with triangular depth profile. $N_1 = 4$, $N_2 = 7$, and $a$ is known

## III. METHOD USING MEASUREMENTS BY A LOOP ANTENNA

### A. Description of the method

In this method, an alternating current $I_s$ with a frequency $f$ is supplied to a conductive wire, positioned close to the flat surface of a metal, generates an induced alternating current $I_i$, with the same frequency, which spreads beneath the surface of the metal. This induced current has a direction opposite to the direction of the supplied current at every moment, its density decreases away from the wire, and its penetration depth beneath the surface of the metal is $\delta = 1/(\pi\mu f\sigma)^{0.5}$, where $\mu$ is the magnetic permeability of the metal and $\sigma$ is its conductivity. Both the supplied current and the induced current generate magnetic fields directed perpendicular to the wire, which could be detected by a loop antenna, positioned as close as possible to the surface of the metal, whose loop is perpendicular to the metal surface and parallel to the wire [3].

The largest contribution to the magnetic field generated by the induced current within the antenna loop, and correspondingly to the voltage measured by the antenna, comes from the induced current path located closest to the antenna, because the magnetic field intensity is inversely proportional to square of the distance between the generation source and the measurement point. This path is named the 'dominant induced current path' (DICP), and in the case of a flat metal surface is parallel to the conductive wire, and located at the metal surface right below the antenna – Fig. 3.

For an alternating current with a frequency $f > 100$ MHz, the induced current spreads within a penetration depth of $\delta < 0.05$ mm beneath the metal surface. Furthermore, the amplitude of the voltage measured by the antenna for a metal surface without cracks can be expressed as follows:

$$|U| \propto |-B_s + B_i| \quad (6)$$

where the two components of the amplitude of the magnetic induction $B_s > 0$ and $B_i > 0$ are generated respectively by the supplied and the induced currents in the region below the antenna loop and have opposite directions at every moment.

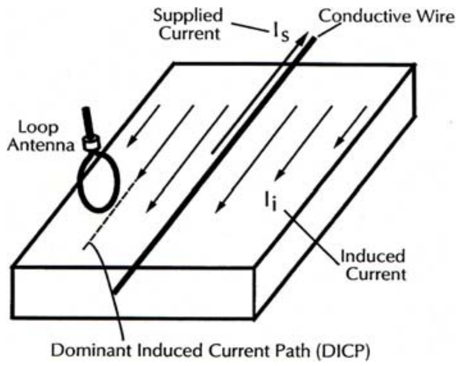


Fig. 3. Geometry, distribution and positioning of the supplied current, the induced current, and the measuring loop antenna

Correspondingly, for a metal surface with cracks, the amplitude of the measured potential drop along the loop of the antenna in the vicinity of a crack is:

$$|U| \propto |-B_s + B_i + B_c| \quad (7)$$

The 'leakage magnetic induction' $B_c > 0$ has the same direction as $B_i$ and is a result of two effects: firstly, a part of the magnetic field generated by the supplied current penetrates into the surface crack. This leads to a decrease of the amplitude of that field within the antenna loop, with respect to a metal surface without cracks, and therefore to a decrease of $B_s$. Secondly, in the vicinity of the crack, the induced current flows within the penetration depth *8* from the crack walls, i.e. it follows the crack geometry closely. The development of such a current bending around the crack leads to reinforcing the magnetic field generated by the induced current, and to increasing $B_i$ – Fig. 4 [4].

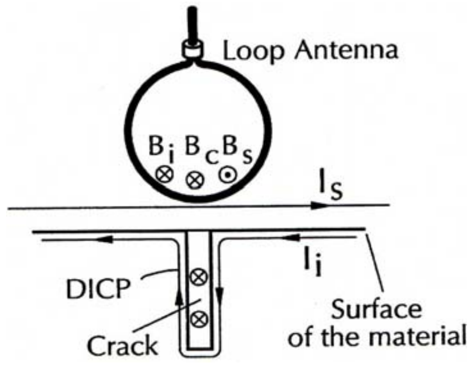


Fig. 4. Illustration of the components of the magnetic induction, with amplitude values $B_s$, $B_i$, and $B_s$ within the antenna loop

For a metal surface without cracks, $B_c = 0$. For a metal surface with cracks, $B_c$ has a larger value for larger cracks, in accordance with the above comments about the meaning of $B_c$. Correspondingly, an analysis of the leakage magnetic induction $B_c$ can provide information about the crack sizes.

*B. Results*

The experiments were performed on a specimen of paramagnetic steel 316. This specimen contained three mechanically cut cracks, having a right angle parallelepiped shape, lengths of 10 mm, widths of 0.15 mm, and depths of correspondingly $d = 0.5$ mm, 1 mm, and 2 mm, whereat the long axes of these cracks were parallel to each other. Cu conductive wire, with a rectangular cross section of 2x0.035 mm, was fixed at a distance of 0.1 mm from the surface of the metal by an insulating plastic foil filling the gap between the specimen and the wire. The long axis ($x$=0,$y$) of the wire was perpendicular to the long axes of the three cracks, and it passed above their geometrical centers. The loop antenna contained a coaxial line with a Cu inner conductor and a Cu shield, as well as a loop with a diameter $D$ which was closed by a solid Cu conductor. The solid Cu conductor was soldered at its two ends correspondingly to the inner conductor of the coaxial line, and to its shield.

The frequency of the supplied sinusoidal voltage was chosen to be $f$ = 300 MHz. A network analyzer was measuring the ratio $R$(dB)=|U|/|$U_s$| between the amplitudes of the voltage at the antenna output and the supplied sinusoidal voltage. The ratio $R$ measured, by a loop antenna with $D$ = 7 mm, along scanning lines ($x$=const,$y$) parallel to the Cu wire, over a surface area of the specimen which contains the cracks, is represented in Fig. 5 for distances $x$ = [2-6] mm from the long axis of the wire. It is seen that, in most cases, the dependences $R$($x$=const,$y$) undergo changes in the vicinity of the cracks, which are most significant at the centers of the cracks, i.e. at $y$ = - 60 mm, 0 mm, and 60 mm. The difference $C = R(x=x_1, y=y_1) - R_f(x=x_1, y=y_1)$, which depends on the crack depth $d$, is named a 'crack response of the ratio $R$' where $R$ and $R_f$ are measured over the same surface area of the specimen when it contains a crack and does not contain a crack, correspondingly. The results shown in Fig. 5 can be explained by an analysis of the behavior of the components of the magnetic inductions in Eq. 7.

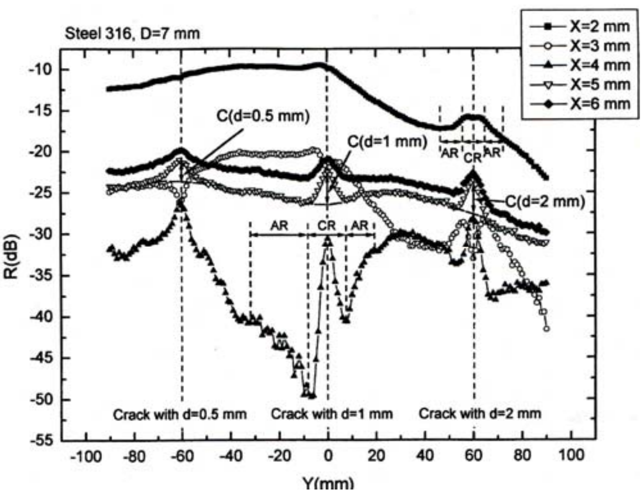


Fig. 5. Ratio $R$ measured by the antenna with $D$ = 7 mm along scanning lines ($x$=const,$y$) over area containing the three cracks

The dependencies of the crack response $C$ measured outside the crack at $x$ = 6 mm on the crack depth $d$ are illustrated in Fig. 6, for loop antennas with 3 different diameters. It is seen that largest $C$ is obtained for the antenna with a diameter $D$ = 7 mm, while best linearity of the dependence $C(d)$ is obtained for diameter $D$ = 10 mm.

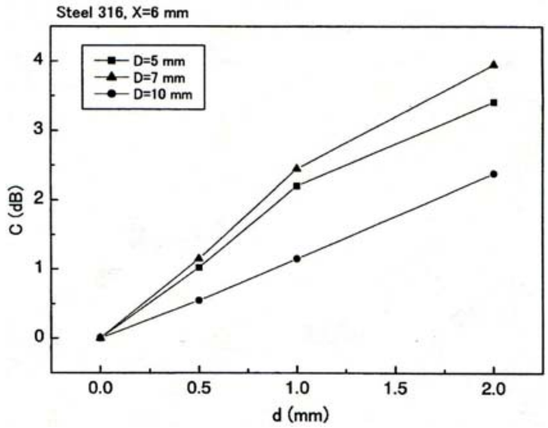


Fig. 6. Dependencies of the crack response $C$ at $x$ = 6 mm on the crack depth $d$, for loop antennas with 3 different diameters

## IV. Conclusion

The obtained results indicate that the method using a Hall element allows simultaneous determination of both the average depth and thickness of a crack. In case that the crack width is measured independently, this method leads to obtaining at least a simplified depth profile. The method using a loop antenna can also provide the average depth of the crack.

The principle of the method using a Hall element has some similarity to that of ultrasonic methods using Rayleigh wave [5], in the sense that the paths of both the magnetic field close to the surface and the Rayleigh wave are influenced by the cracks, which leads to a change in the output signal. The Hall element method though allows extracting information about the width and the shape of the crack, unlike the method from [5].

The method using a loop antenna has some similarity to resonant methods using scanning waveguides [6], because all of these methods employ a scanning probe operated at microwave frequency. These methods can detect cracks with sub-mm depths, but the loop antenna method uses frequency of only 300 MHz, while the method from [6] uses frequency of above 8 GHz and inconvenient filling the cracks with dielectric material.

## References

[1] D. Minkov, J. Lee, T. Shoji, Journal of Magnetism and Magnetic Materials, 217(2000)207-215.

[2] D. Minkov, Y. Takeda, T. Shoji, J. Lee, Applied Physics A, 74(2002)169-176.

[3] T. Shoji, Y. Sato, D. Minkov, K. Yagi, T. Baba, K. Tamakawa, International Journal of Applied Electromagnetics and Mechanics, 14(2001/2002)467-476.

[4] K. Yagi, N. Sato, Y. Sato, K. Tamakawa, D. Minkov, T. Shoji, Applied Physics A, 77(2003)461-468.

[5] V. M. Ushakov, D. M. Davydov, L. I. Domozhirov, Russian Journal of non-destructive testing, 47(2011)631-641.

[6] A. McClanahan, S. Kharkovsky, A. R. Maxon, R. Zoughi, D. D. Palmer, IEEE Transactions on Instrumentation and Measurement, 59(2010),1693-1704.